The Effect of Temperature Rise of the Fuzzy Logic-Controlled Braking Resistors on Transient Stability

Mohd. Hasan Ali, *Student Member, IEEE*, Toshiaki Murata, and Junji Tamura, *Senior Member, IEEE*

***Abstract*—Braking resistor is a very powerful tool to improve transient stability in a power system. Usually, a fixed value of the braking resistor is considered for the transient stability analysis. However, when the braking resistor is in operation, temperature of the resistor material rises above ambient temperature which ultimately causes the resistance value to increase. This paper analyzes the effect of the temperature rise of the fuzzy logic-controlled braking resistor on the transient stability in a multimachine power system. The performance of the braking resistor scheme with fuzzy controller is compared to that of with conventional proportional-integral-derivative (PID) controller. Simulation results of both balanced and unbalanced faults at different points in the system indicate that the temperature rise of the fuzzy logic-controlled braking resistors has little or almost no effect on the transient stability of the multimachine power system. Moreover, it is found that the performance of fuzzy logic controller is better than that of conventional PID controller. Thus, the proposed fuzzy control strategy provides a simple and effective method of transient stability enhancement.**

***Index Terms*—Balanced and unbalanced faults, braking resistor, EMTP, fuzzy logic controller, genetic algorithm, PID controller, temperature rise effect, transient stability.**

I. Introduction

BRAKING resistor (BR) is known to be a very effective device for transient stability control. It can be viewed as a fast load injection to absorb excess transient energy of an area which arises due to severe system disturbances. Again, fuzzy logic is a powerful problem-solving methodology with a myriad of applications in embedded control and information processing. Fuzzy provides a remarkably simple way to draw definite conclusions from vague, ambiguous, or imprecise information. In a sense, fuzzy logic resembles human decision making with its ability to work from approximate data and find precise solutions. The control method of modeling human language has many advantages, such as simple calculation, as well high robustness, lack of a need to find the transfer function of the system, suitability for nonlinear systems, etc. [1].

Exploiting the concept of fuzzy logic, we proposed the works [2]–[5] for the switching of the thyristor-controlled braking resistor to improve power system transient stability. However, in all of these works, a fixed value of the braking resistor is considered and temperature rise effect of the braking resistor is neglected. But practically, when the braking resistor is in operation, temperature of the braking resistor material rises above ambient temperature and, hence, its resistance value increases. Consequently, higher temperature may cause the resistor material to melt away and due to higher resistance value, the system response may be somewhat affected. So, the temperature rise phenomenon of the braking resistor should be included for the actual analysis of transient stability.

The novel feature of this paper is that it analyzes the effect of the temperature rise of the fuzzy logic-controlled braking resistor on transient stability in a multimachine power system. The performance of the braking resistor scheme with fuzzy controller is compared to that of with conventional PID controller. Another salient feature of this work is that the input to the fuzzy or PID controllers is the deviation of the total kinetic energy of the system instead of the local speed deviation of each generator as used in our previous works [2]–[5]. The total kinetic energy of the system has also been utilized as an index for the transient stability evaluation. The controller parameters are optimally tuned by the genetic-algorithm (GA) technique [1], [2]. Moreover, the Institute of Electrical Engineers of Japan (IEEJ) West 10-machine model system [6] instead of single machine system [4], [5] and three-machines system [2], [3] as those used in our previous works has been taken into account in the present work.

The organization of this paper is as follows: Section II describes the model system for the analysis of transient stability. Section III describes the temperature rise phenomenon of the braking resistor. Section IV explains the proposed fuzzy controller design. In Section V, design of the conventional PID controller is explained. Section VI describes the tuning procedure of the controller parameters by the GA technique. Section VII describes the simulation results. Finally, Section VIII provides some conclusions regarding the proposed control strategy.

II. Model System

The IEEJ West 10-machine model system [6] as shown in Fig. 1 has been used in the present work for the simulation of transient stability. The model system has ten generators G1 to G10 as shown in Fig. 1. Generator G10 is considered as the swing generator in the system. The braking resistor BR with a conductance value of G_{TCSBR} is connected to the high tension side of each step up transformer through the thyristor switching circuit, as shown in Fig. 2 where G indicates any of the generators from G1 to G10. The conductance values of the braking

Manuscript received September 17, 2003.

The authors are with the Department of Electrical and Electronic Engineering, Kitami Institute of Technology, Hokkaido 090-8507, Japan (e-mail: hasan@pullout.elec.kitami-it.ac.jp).

Digital Object Identifier 10.1109/TPWRS.2004.825828

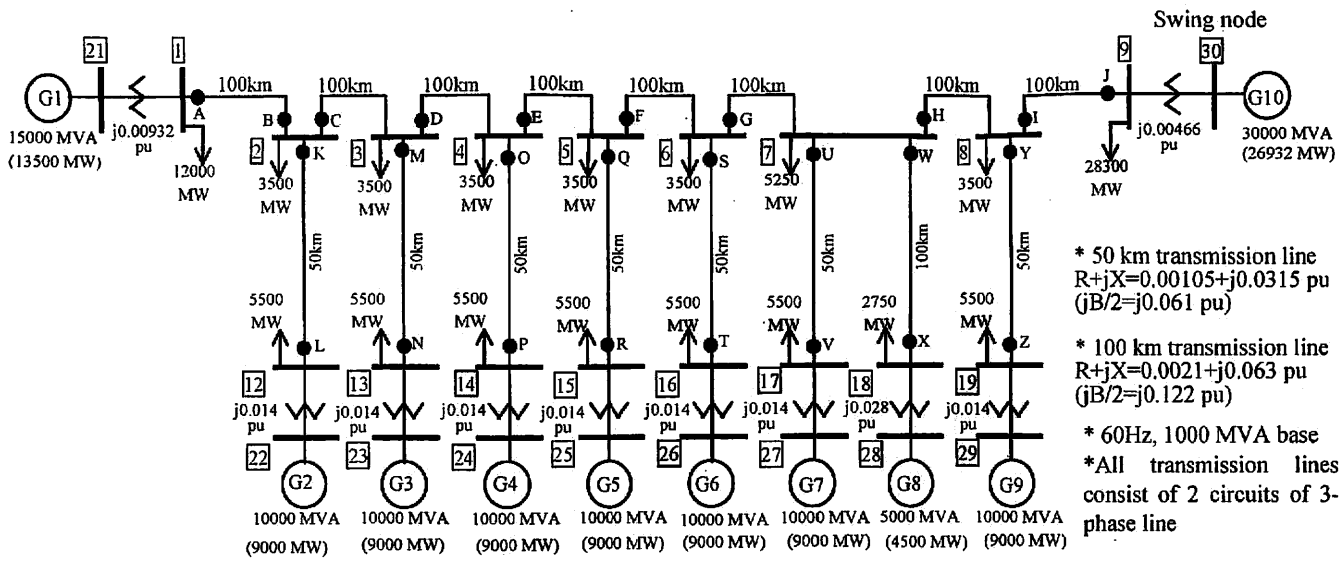

Fig. 1. IEEJ West 10-machine model system.

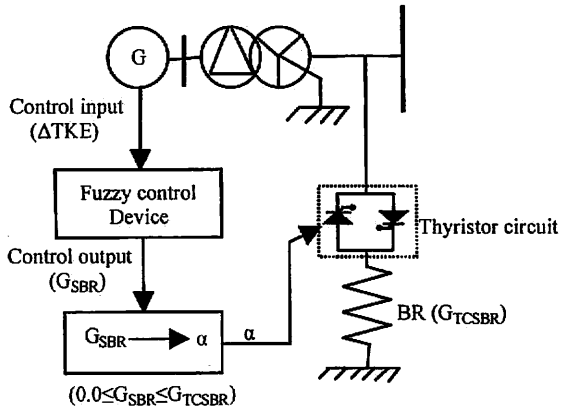

Fig. 2. BR with thyristor switching circuit.

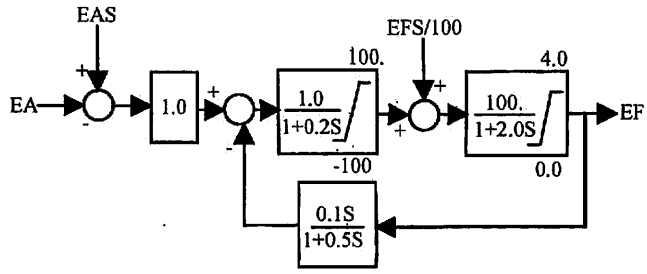

Fig. 3. IEEJ AVR model (LAT = 1).

resistors are selected from the viewpoint that they can absorb an amount of power equal to the rated capacity of the machines at full conduction, if the voltage across the resistor is about 1.0 p.u. [2]–[5]. The system base is 1000 MVA. Therefore, the conductance values of the braking resistors BR1, BR2–BR7 and BR9, BR8, and BR10 are considered 15.0 p.u., 10.0 p.u., 5.0 p.u., and 30.0 p.u., respectively. The BR will be switched in following a fault clearing and the switching condition of BR is such that when deviation of total kinetic energy ΔTKE of the generators exceeds 0.2 p.u., BR is switched on the generator terminal bus. On the other hand, when ΔTKE is below or equal to 0.2 p.u., and also in the steady state, BR is removed from the generator terminal bus by the thyristor switching circuit. The dead band of the BR operation (i.e., the threshold value of ΔTKE) is determined by trial and error. The automatic voltage regulator (AVR) and Governor (GOV) control system models for the IEEJ West 10-machine model system [6] have been included in the present simulation and are shown in Figs. 3 and 4, respectively. Table I shows the various parameters of the generators [6] used for the simulation. The generator parameters in Table I are based on the machine ratings.

III. Calculation of Temperature Change and Resistance Change Values of Braking Resistor

When the braking resistor is in operation, temperature of the resistor material rises above ambient temperature and, hence, its resistance value increases. To calculate the amount of temperature rise for a time duration, heat exchange coefficient, specific heat, mass, and surface area of the braking resistor material with a particular resistance value should be known. This is explained below.

A braking resistor is a passive device which converts electrical energy into heat. It is expressed mathematically as follows:

$$E = RI^2t \tag{1}$$

where E = energy injected into the braking resistor, I = current through the braking resistor and t = time duration.

The energy injected into the braking resistor can also be expressed as [7]

$$E = E_S + E_D \tag{2}$$

where E_S is energy stored into the braking resistor and E_D is energy dissipated from the braking resistor.

E_S and E_D are related to the physical characteristics of the braking resistor as follows:

$$E_S = CM\Delta T \tag{3}$$

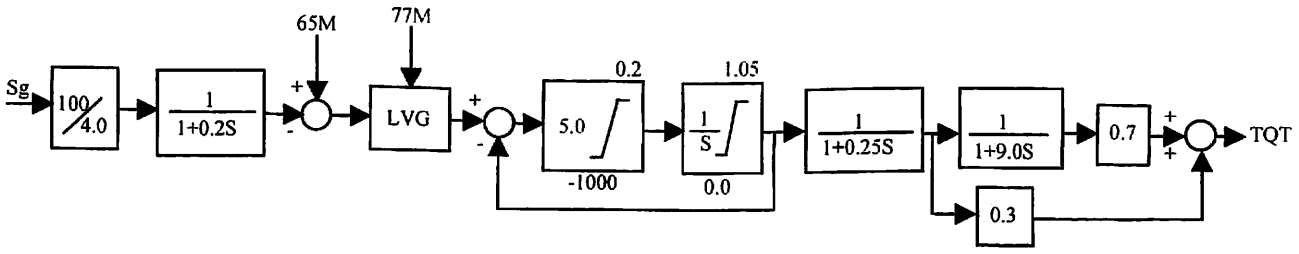

Fig. 4. IEEJ GOV model (LPT = 1).

TABLE I
GENERATOR PARAMETERS

X_d [pu]	1.70	T_d'' [sec]	0.03
X_q [pu]	1.70	T_q'' [sec]	0.03
X_d' [pu]	0.35	T_a [sec]	0.40
X_d'' [pu]	0.25	X_l [pu]	0.225
X_q'' [pu]	0.25	H [sec]	7.00
T_d' [sec]	1.00		

where C is specific heat of the braking resistor material and is dependent on temperature, M is the mass of the braking resistor, and ΔT is the temperature rise above ambient and

$$E_D = KS\Delta T \tag{4}$$

where K is the heat exchange coefficient and is dependent on the geometry of the braking resistor and on temperature and S is the surface area of the braking resistor.

Therefore, assuming that heating is nonadiabatic, temperature rise of the braking resistor above ambient is given by

$$\Delta T = \frac{RI^2t}{(CM + KS)}. \tag{5}$$

Therefore, from (5), the amount of temperature rise of the braking resistor material can be calculated. In this work, we have considered that the material for the braking resistor is stainless steel which has an upper temperature limit of 800 °C, a temperature coefficient of resistance of 0.001, a specific heat of 500 J/°C/kg at 20 °C of ambient temperature [7]. For free convection in air, the typical value of heat exchange coefficient is 5–25 W/m^2 ·° C [8]. In this work, we have used the value of heat exchange coefficient of 25 W/m^2 ·° C.

Now it is seen that although all of the variables are known to calculate the amount of temperature rise using (5) for a time duration, mass and surface area of the braking resistor material are not known. For a fixed resistance value of a particular material, its mass and surface area may be different. Again, temperature rise is affected by variable masses and surface areas as will be shown in the simulation results later. Also, depending on variable masses and surface areas, size and, hence, cost of the braking resistor will vary. So, the braking resistor should be designed properly so that the material does not melt away because of its higher temperature rise as well as the cost and size of the braking resistor are reasonable. In this work, extensive simulations are carried out considering variable values of masses and surface areas of the braking resistor.

The initial resistance values of the braking resistors BR1, BR2–BR7 and BR9, BR8, and BR10 are 16.67 ohm, 25.0 ohm, 50.0 ohm, and 8.33 ohm, respectively. When the temperature of the braking resistor increases, the resistance value also increases according to the following formula [7]:

$$R_t = R_0(1 + \gamma\Delta T) \tag{6}$$

where R_t = resistance at time t, R_0 = initial resistance, γ = temperature coefficient of resistance and ΔT = temperature rise.

When the braking resistor is not in the circuit, it gets cooled down by dissipating heat into the air. Therefore, temperature of the resistor and, hence, resistance value decrease exponentially. According to Newton's law of cooling, the temperature decrease can be calculated from the following equation [9]:

$$T(t) = T_a + (T_0 - T_a)e^{-nt} \tag{7}$$

where $T(t)$ = temperature of the braking resistor at time t, T_a = ambient temperature (20°C), T_0 = initial temperature of the braking resistor and n = positive constant (0.1 for this work).

Again, when the braking resistor is not in the circuit, resistance decrease value can be calculated from the following equation:

$$R_t = R_0(1 - \gamma\Delta T). \tag{8}$$

IV. DESIGN OF FUZZY LOGIC CONTROLLER

The design of the proposed fuzzy logic controller (FLC) is described in the following:

A. Fuzzification

For the design of the proposed FLC, deviation of total kinetic energy ΔTKE of the generators and conductance value of BR, G_{SBR} ($0.0 \le G_{SBR} \le G_{TCSBR}$) are selected as the input and output, respectively. The use of single input and single output variable makes the design of the controller very straightforward [2]–[5]. In [2]–[5], we selected the deviation of speed of the generator as the input to the fuzzy controller. However, the reason for the selection of the deviation of total kinetic energy as the input to the fuzzy controller in this work is explained in Section VII-A. We have selected the triangular membership functions for ΔTKE as shown in Fig. 5 in which the linguistic variables NE, ZO, and PO stand for negative, zero, and positive, respectively. It is important to note that the membership functions are the same for each fuzzy controller.

B. Fuzzy Rule Table

The proposed control strategy is very simple because it has only three control rules for each controller as shown in Table II

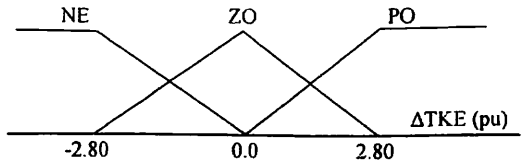

Fig. 5. Membership function of ΔTKE.

TABLE II
FUZZY RULE TABLE

ΔTKE	G_{SBR}[pu]									
	BR1	BR2	BR3	BR4	BR5	BR6	BR7	BR8	BR9	BR10
NE	0.0	0.0	0.0	0.0	0.0	0.0	0.0	0.0	0.0	0.0
ZO	0.0	0.0	0.0	0.0	0.0	0.0	0.0	0.0	0.0	0.0
PO	15.0	10.0	10.0	4.0	4.0	4.0	0.1	0.1	0.1	4.0

where the numerical values of G_{SBR} given with respect to system base power represent the output of the fuzzy controller.

C. Fuzzy Inference and Defuzzification

For the inference mechanism of the proposed fuzzy logic controller, Mamdani's method [10] has been utilized. Again, the center-of-area method is the most well known and rather simple defuzzification method [10] which is implemented to determine the output crispy value (i.e., the conductance value of the braking resistor G_{SBR}).

V. Design of PID Controller

The classical PID controller finds extensive application in industrial control. The block diagram of the continuous-time PID controller is shown in Fig. 6. The transfer function of the classical PID controller used in this simulation is written in s-domain as the following [11]:

$$G_{SBR} = K_p\left(1 + \frac{1}{T_i s} + T_d s\right)\Delta TKE \tag{9}$$

where G_{SBR} and ΔTKE represent the input and output variables of the controller, respectively, and bear the same meanings as explained in Section IV. K_p, T_i, and T_d represent the proportional gain, integration time constant, and derivative or rate time constant, respectively.

The values of K_p, T_i, and T_d used in this work are shown in Table III. It is important to note that the same parameters are used for each controller throughout the simulations.

VI. Tuning of the Controller Parameters by GA

Usually, the fuzzy logic controller parameters as well as PID controller parameters are determined by trial and error which is cumbersome and time consuming. Therefore, to surmount such a drawback, in this work, we have applied the GA technique [1], [2] for optimal tuning of fuzzy and PID controller parameters.

GAs are search procedures and optimization techniques based on the mechanics of natural selection and natural genetics [12]. Before a GA is applied, the optimization problem should be converted to a suitably described function called "Fitness Function." It represents a performance of the problem. The higher the fitness value, the better the system's performance.

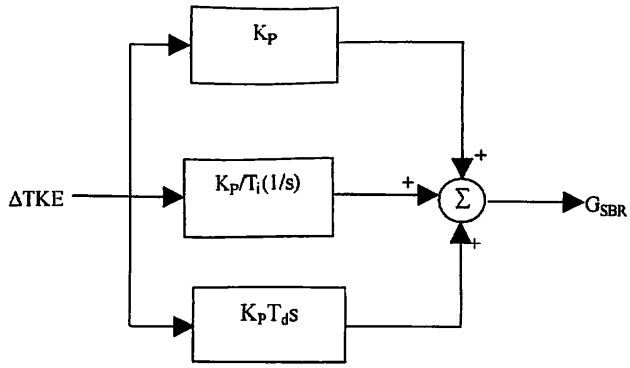

Fig. 6. Block diagram of PID controller.

TABLE III
PARAMETERS OF PID CONTROLLER

K_P	T_i	T_d
4.0	0.4	0.02

In this work, the integral of the absolute value of the time derivative of total kinetic energy divided by the system base power is selected as the objective function. Therefore, the objective function Obj is expressed simply as

$$Obj = \int_0^T \left|\frac{d}{dt}W_{\text{total}}\right| dt/\text{system base power} \tag{10}$$

which is to be minimized and where T is the simulation time of 10.0 s, W_{total} is the total kinetic energy which can be calculated easily by knowing the rotor speed of each generator and is given by

$$W_{\text{total}} = \sum_{i=1}^{N} W_i\,(J) \tag{11}$$

where

$$W_i = \frac{1}{2}J_i{\omega_{mi}}^2\,(J) \tag{12}$$

denotes kinetic energy in joule for a generator, W_{total} total kinetic energy in joule, i is generator number, and N total number of generators. Again, in (12), J_i denotes the moment of inertia in Kg.m^2 and ω_{mi} rotor angular velocity in mechanical radians per second.

The corresponding fitness function Fit is given by

$$\text{Fit} = \frac{1}{Obj}. \tag{13}$$

To apply the GA technique in this work, at first 30 sets of individuals or chromosomes each consisting of 11 discrete real-coded genes (for fuzzy controller) or three discrete real-coded genes (for PID controller) are generated as the initial population from the point of view of system knowledge.

Next, the GA involves two basic steps: i) the system is simulated to calculate the fitness function and ii) three operations are performed: Selection or Reproduction, Crossover and Mutation

to produce the next generation of individuals. The techniques of **Selection**, **Crossover** and **Mutation** used in this work are roulette wheel selection, single point crossover, and nonuniform mutation [13], respectively.

The above two steps are repeatedly applied until convergence condition is satisfied, producing a near optimal parameter set. Finally, the membership functions and control rules of the optimal FLC as well as PID controller parameters as developed by the GA are already shown in Fig. 5, Table II, and Table III, respectively.

The firing control signal can be determined from the conductance value G_{SBR} and then sent to the thyristor switching unit to modify the real power absorbed by the braking resistor in the transient condition. The modeling of thyristor-controlled system braking resistor (TCSBR) and method of calculating firing-angle from the output of the fuzzy or PID controller are described in detail in [3]–[5].

VII. Simulation Results and Discussion

In the simulation study, 26 fault points from A-Z as shown in the model system of Fig. 1 have been considered. In all of the cases, the fault occurs at 0.1 s, the circuit breakers on the faulted lines are opened at 0.17 s, and at 1.003 s the circuit breakers are closed. Time step and simulation time have been chosen as 0.000 05 s and 10.0 s, respectively.

A. Impact of Using Total Kinetic Energy as Input to Fuzzy Controller

In this work, at first simulations were carried out considering both balanced [three-phase-to-ground (3LG)] and [unbalanced single-line-to-ground a-phase (1LG)] faults at different points on the transmission lines without taking the temperature rise effect of the BR into account. Deviation of speed of the generator was considered as the input to the fuzzy controller at first. But the system was not found to be stable for all fault points, that is, at some fault points, the system was stable and at some fault points, the system was unstable. Since the overall system was not found to be stable using local variable (i.e., deviation of speed of each generator) as the input to each controller, the need for a global variable as a common input to each controller is stressed and from this viewpoint, deviation of total kinetic energy is finally thought to be the input to each fuzzy controller. By using deviation of total kinetic energy of the generators as the input to the fuzzy controller, we have observed that the system is transiently stable at all fault points for the fault clearing time of 70 ms.

However, a question may arise regarding the online calculation of the total kinetic energy using the speed signal of each generator and then again using deviation of total kinetic energy signal as the input to each fuzzy or PID controller. But this can be accomplished by using global positioning system (GPS) [14]–[16] which provides time synchronization of signals. It has recently been recognized that synchronized measurement of power system quantities is feasible using the GPS, since GPS can easily and precisely provide a time signal, with a 1-μs accuracy, at any location on the power network [15]. Fig. 7

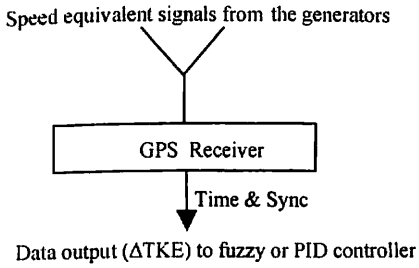

Fig. 7. GPS functional block diagram.

shows a simplified functional block diagram where the GPS receiver collects the speed signals from the generators, synchronizes the signals in a common timing reference, and calculates W_{total}. Data output (i.e., the signal of ΔTKE) is then sent to each fuzzy or PID controller as the input. In this case, signals may be transmitted and received through optical fiber.

B. Usage of Total Kinetic Energy as the Stability Index

For the evaluation of transient stability, in this work, we have used the stability index W_c [17] given by

$$W_c(\text{sec}) = \int_0^T \left| \frac{d}{dt} W_{\text{total}} \right| dt / \text{system base power} \qquad (14)$$

where T is the simulation time selected to 10.0 s. Actually, the right-hand side of (14) is the same as that of (10). The smaller the value of W_c, the better the system's performance.

Taking the deviation of total kinetic energy as the input to fuzzy and PID controllers, the values of W_c for 3LG and 1LG faults at all points with BR as well as without BR are calculated without considering the temperature rise effect of BR and shown in Table IV. From Table IV, it is seen that the value of W_c is the highest at point A in the case when there is no BR for both fault cases. Also, we observed the load angle responses at all fault points without BR and it was found that the load angle responses for the fault at point A are the worst. From this viewpoint, point A can be considered as the severest fault point in the system. Moreover, a 3LG fault on the transmission line is the severest in a power system. Therefore, the fuzzy and PID controller parameters are tuned with respect to a 3LG fault at point A and then the same fuzzy and PID controller parameters are used throughout the simulations for all types of faults and fault points. Also, from the values of W_c, the effectiveness of the fuzzy logic-controlled braking resistor and that of PID controlled braking resistor in enhancing transient stability irrespective of fault point is clearly seen. However, it is observed that the performance of fuzzy controller is better than that of PID controller. This fact corroborates the superiority of the proposed fuzzy logic-controlled braking resistor in enhancing transient stability over PID-controlled BR.

Figs. 8–13 show the load angle responses in case of 3LG and 1LG faults at point A for both fuzzy and PID-controlled BR without considering the temperature rise effect of BR. The load angles for the generators are calculated with respect to the load angle of the swing generator G10 in the model system. From the load angle responses, it is observed that the system is transiently stable because of the use of BR. Moreover, from the point

TABLE IV
VALUES OF W_c WITH AND WITHOUT BR

Fault point	Values of W_c for 3LG fault			Values of W_c for 1LG fault		
	fuzzy controlled BR	PID controlled BR	without BR	fuzzy controlled BR	PID controlled BR	without BR
A	23.70	27.74	104.50	15.32	15.39	31.66
B	12.12	13.95	54.71	8.93	9.31	19.68
C	18.52	19.01	57.66	8.14	9.35	19.27
D	9.04	10.58	27.04	4.14	4.59	11.70
E	16.0	16.92	17.08	6.61	6.64	7.43
F	17.55	19.41	25.20	9.76	10.25	10.51
G	22.58	28.76	33.31	8.85	10.21	13.12
H	26.74	32.58	37.75	11.70	13.51	15.45
I	24.13	25.43	27.52	8.52	10.21	12.96
J	32.08	35.40	56.72	21.64	22.21	24.69
K	10.0	12.40	88.31	8.70	9.56	20.80
L	13.97	15.53	79.78	10.02	11.80	24.23
M	9.14	12.89	34.02	4.16	4.70	12.73
N	9.72	9.87	34.33	5.85	6.43	14.88
O	16.4	17.53	18.02	5.89	6.93	7.71
P	17.78	17.94	18.55	7.10	8.34	9.02
Q	19.12	21.66	25.69	8.98	10.42	10.77
R	18.78	20.48	25.90	10.75	12.12	12.33
S	20.21	22.89	33.62	8.82	9.99	13.48
T	18.96	20.78	34.70	8.60	9.91	15.02
U	32.49	36.0	38.65	12.08	13.88	15.85
V	28.71	33.36	35.91	10.24	11.92	15.73
W	27.75	32.02	35.18	12.20	13.42	15.58
X	15.83	17.50	22.32	5.97	6.91	9.97
Y	22.00	26.22	29.56	8.60	10.68	13.33
Z	22.76	25.93	27.98	10.19	11.64	13.55

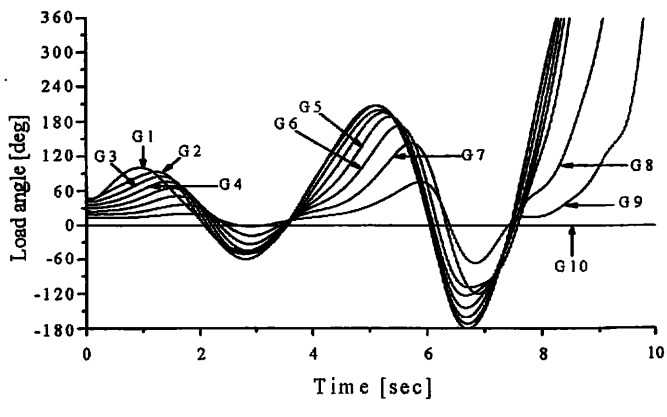

Fig. 8. Load angle responses for 3LG fault at point A (without BR).

of view of oscillation, the performance of the fuzzy logic-controlled BR is better than that of PID controlled BR for both balanced and unbalanced fault conditions.

C. Effect of Temperature Rise of BR on Transient Stability

In this work, considering temperature rise of the braking resistors, extensive simulations were carried out for variable

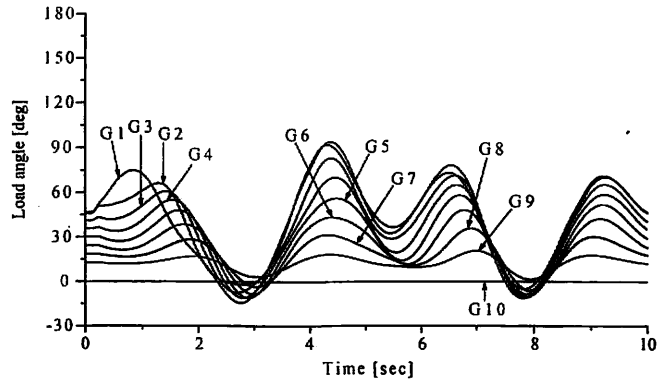

Fig. 9. Load angle responses for fuzzy-controlled BR in case of 3LG fault at point A (without temperature rise effect).

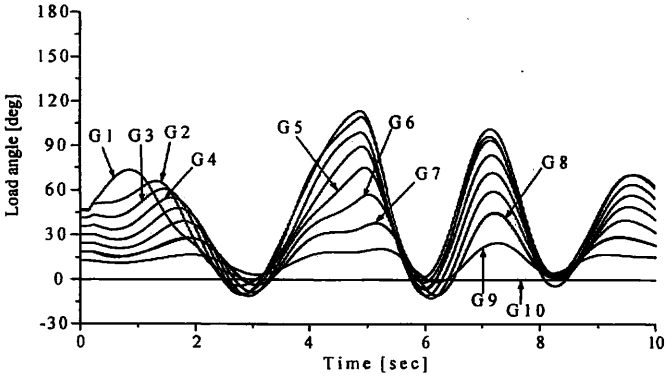

Fig. 10. Load angle responses for PID-controlled BR in case of 3LG fault at point A (without temperature rise effect).

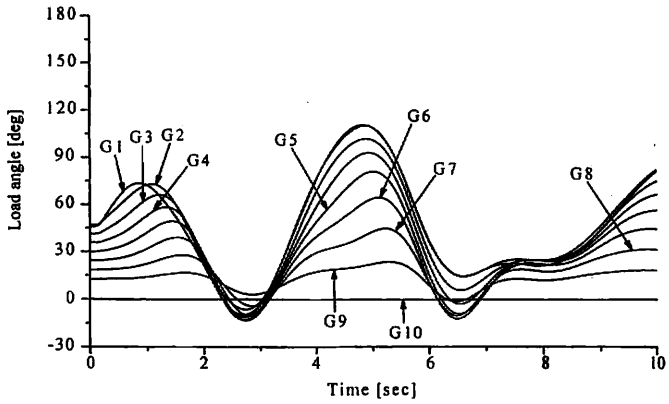

Fig. 11. Load angle responses for 1LG fault at point A (without BR).

values of masses and surface areas of the resistor material. Some of the simulation cases for variable values of masses and surface areas are shown in Table V. Tables VI–IX show the values of maximum temperature rise, maximum resistance rise, as well as values of Wc corresponding to the simulation cases as shown in Table V for both fuzzy and PID-controlled braking resistors in case of 3LG and 1LG faults at point A.

Some of the salient features which we observe from the simulation results of Tables VI–IX are shown.

i) In case of both 3LG and 1LG faults, the maximum temperature rise is well within the upper temperature limit of 800 °C for stainless steel for variable values of

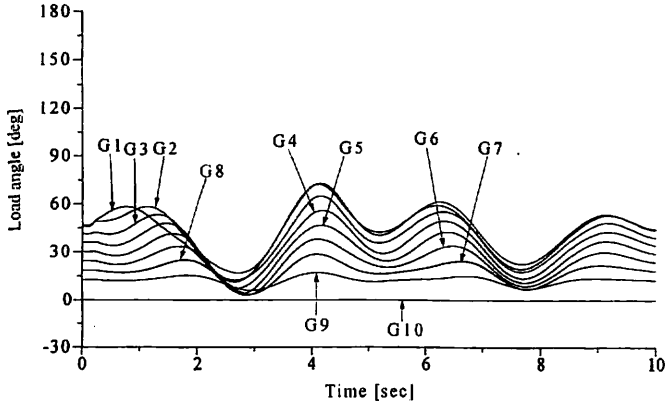

Fig. 12. Load angle responses for fuzzy-controlled BR in case of 1LG fault at point A (without temperature rise effect).

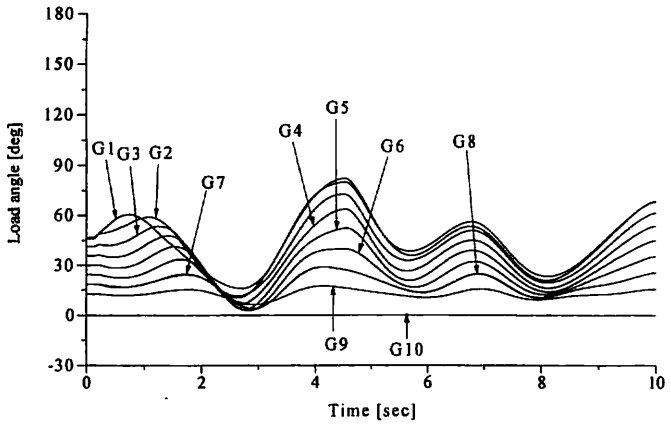

Fig. 13. Load angle responses for PID-controlled BR in case of 1LG fault at point A (without temperature rise effect).

masses and surface areas of both fuzzy and PID-controlled braking resistors. However, from the values of Wc, the superior performance of fuzzy-controlled BR over PID-controlled BR is clearly seen.

ii) The difference among the values of Wc for both fuzzy and PID controlled BR as shown in Tables VI–IX and those of for both fuzzy and PID-controlled BR as shown in Table IV for the fault at point A is small. This signifies that the temperature rise has little or almost no effect on transient stability.

iii) In case of both 3LG and 1LG faults, it is observed for both fuzzy and PID-controlled BR that with the increase of masses and surface areas, temperature and resistance values decrease. Higher temperature rise of the resistor material is not desirable, because higher temperature may cause the resistor material to melt away. In this sense, large mass and surface area of the braking resistor is better. But with the increase of mass and surface area, size and, hence, cost of the braking resistor will increase. Therefore, although the objective of this work is not to design the braking resistor, it may be emphasized that the masses and surface areas of the braking resistors should be such that the temperature rise is well within the upper temperature limit of the material, it is reasonable in size and cost-effective.

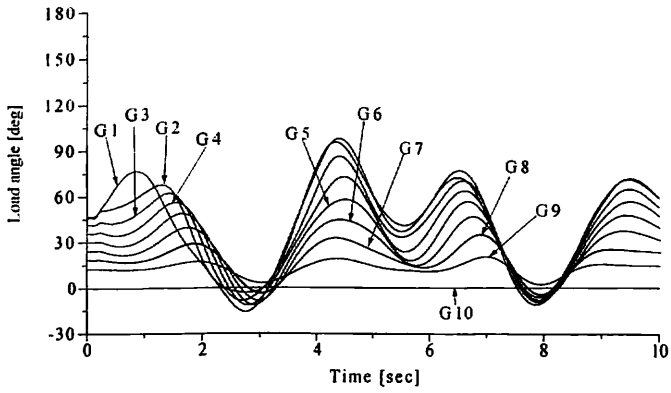

Fig. 14. Load angle responses for fuzzy-controlled BR in case of 3LG fault at point A (simulation case 1 when temperature rise effect is considered).

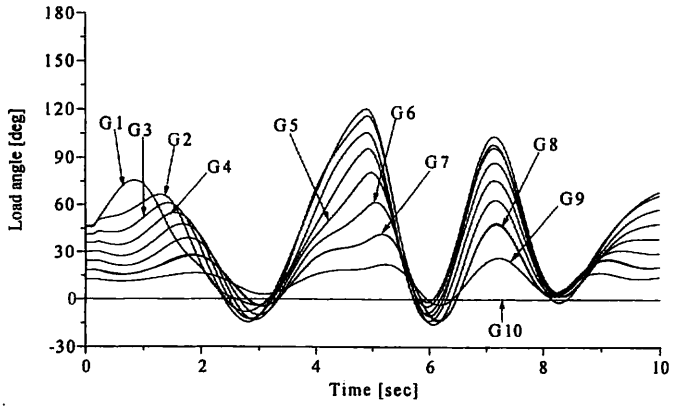

Fig. 15. Load angle responses for PID controlled BR in case of 3LG fault at point A (simulation case 1 when temperature rise effect is considered).

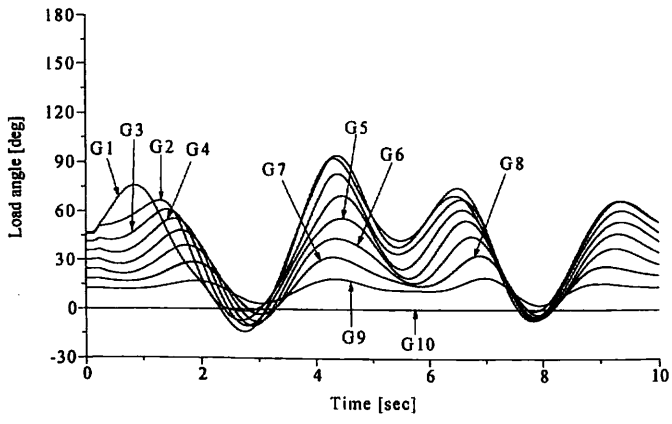

Fig. 16. Load angle responses for fuzzy-controlled BR in case of 3LG fault at point A (simulation case 6 when temperature rise effect is considered).

Figs. 14–21 show the load angle responses in case of 3LG and 1LG faults at point A for the simulation cases 1 and 6 of Table V. From these responses, it is seen that the load angle responses for the simulation case 1 in case of both fuzzy and PID-controlled BR are almost the same as those for the simulation case 6 in case of both fuzzy and PID-controlled BR. Moreover, there is no significant difference among the load angle responses as shown in Figs. 9, 10, 12, and 13 without considering temperature rise of both fuzzy and PID-controlled BR and those of,

TABLE V
SIMULATION CASES FOR VARIOUS MASSES AND SURFACE AREAS OF BR

	BR1	BR2	BR3	BR4	BR5	BR6	BR7	BR8	BR9	BR10	Case no.
Mass [kg]	2500	2000	2000	2000	2000	2000	2000	1000	2000	5000	1
Surface area [m^2]	1.5	1.0	1.0	1.0	1.0	1.0	1.0	0.5	1.0	2.0	
Mass [kg]	5000	4000	4000	4000	4000	4000	4000	2000	4000	10000	2
Surface area [m^2]	2.0	1.5	1.5	1.5	1.5	1.5	1.5	1.0	1.5	2.5	
Mass [kg]	8000	6000	6000	6000	6000	6000	6000	3000	6000	16000	3
Surface area [m^2]	2.5	2.0	2.0	2.0	2.0	2.0	2.0	1.5	2.0	3.0	
Mass [kg]	10000	8000	8000	8000	8000	8000	8000	4000	8000	20000	4
Surface area [m^2]	3.0	2.5	2.5	2.5	2.5	2.5	2.5	2.0	2.5	3.5	
Mass [kg]	12000	10000	10000	10000	10000	10000	10000	5000	10000	24000	5
Surface area [m^2]	3.5	3.0	3.0	3.0	3.0	3.0	3.0	2.5	3.0	4.0	
Mass [kg]	15000	12000	12000	12000	12000	12000	12000	6000	12000	30000	6
Surface area [m^2]	4.0	3.5	3.5	3.5	3.5	3.5	3.5	3.0	3.5	5.0	

TABLE VI
VALUES OF MAXIMUM TEMPERATURE RISE, MAXIMUM RESISTANCE RISE, AND Wc FOR FUZZY-CONTROLLED BR WHEN 3LG FAULT OCCURS AT POINT A

	BR1	BR2	BR3	BR4	BR5	BR6	BR7	BR8	BR9	BR10	Value of Wc	Case no.
Max. temp. [^{0}C]	310.0	255.0	210.0	136.0	95.0	60.0	24.8	27.0	22.75	47.1	24.24	1
Max. res. [ohm]	22.3	31.7	30.3	28.1	26.9	26.0	25.12	50.35	25.07	8.57		
Max. temp. [^{0}C]	165.0	140.0	114.0	78.0	57.5	41.0	22.5	23.5	21.4	30.3	24.26	2
Max. res. [ohm]	19.25	28.25	27.5	26.5	25.9	25.52	25.06	50.18	25.04	8.42		
Max. temp. [^{0}C]	110.0	98.0	82.0	57.5	45.0	33.8	21.7	22.4	20.9	26.0	24.26	3
Max. res. [ohm]	18.2	27.0	26.6	25.9	25.6	25.34	25.04	50.12	25.02	8.38		
Max. temp. [^{0}C]	92.0	79.0	66.0	48.0	38.0	30.0	21.3	21.8	20.7	24.6	24.36	4
Max. res. [ohm]	17.9	26.5	26.2	25.7	25.45	25.25	25.03	50.09	25.02	8.36		
Max. temp. [^{0}C]	80.0	67.0	57.5	42.0	35.0	28.2	21.0	21.4	20.5	23.7	24.42	5
Max. res. [ohm]	17.7	26.2	25.9	25.58	25.37	25.20	25.02	50.07	25.0	8.36		
Max. temp. [^{0}C]	68.0	60.0	52.0	38.0	32.4	26.8	20.8	21.2	20.48	22.9	24.42	6
Max. res. [ohm]	17.5	26.0	25.8	25.50	25.30	25.12	25.02	50.06	25.0	8.36		

TABLE VII
VALUES OF MAXIMUM TEMPERATURE RISE, MAXIMUM RESISTANCE RISE, AND Wc FOR PID-CONTROLLED BR WHEN 3LG FAULT OCCURS AT POINT A

	BR1	BR2	BR3	BR4	BR5	BR6	BR7	BR8	BR9	BR10	Value of Wc	Case no.
Max. temp. [^{0}C]	375.0	350.0	310.0	250.0	190.0	120.0	72.0	117.0	71.0	74.0	27.60	1
Max. res. [ohm]	23.8	35.0	33.2	31.5	29.5	27.5	26.3	55.0	26.3	8.8		
Max. temp. [^{0}C]	220.0	190.0	164.0	135.0	100.0	68.0	45.0	70.0	45.0	45.0	28.56	2
Max. res. [ohm]	20.0	29.6	28.8	28.1	27.2	26.2	25.65	52.6	25.65	8.55		
Max. temp. [^{0}C]	132.0	132.0	115.0	96.0	73.0	52.0	37.0	57.0	38.0	35.5	28.97	3
Max. res. [ohm]	18.54	28.0	27.5	27.0	26.3	25.8	25.45	51.7	25.45	8.46		
Max. temp. [^{0}C]	110.0	104.0	92.0	77.0	60.0	43.0	33.0	47.0	33.0	32.5	29.18	4
Max. res. [ohm]	18.3	27.3	26.8	26.5	26.0	25.6	25.33	51.4	25.34	8.43		
Max. temp. [^{0}C]	100.0	91.0	80.0	68.0	54.0	40.0	31.0	44.0	31.8	31.0	29.68	5
Max. res. [ohm]	18.1	26.7	26.5	26.2	25.9	25.52	25.27	51.2	25.28	8.42		
Max. temp. [^{0}C]	80.0	77.0	68.0	56.0	47.0	36.0	30.2	55.0	31.0	27.9	29.52	6
Max. res. [ohm]	17.7	26.4	26.2	26.0	25.7	25.4	25.26	51.8	25.27	8.40		

TABLE VIII
VALUES OF MAXIMUM TEMPERATURE RISE, MAXIMUM RESISTANCE RISE, AND Wc FOR FUZZY-CONTROLLED BR WHEN 1LG FAULT OCCURES AT POINT A

	BR1	BR2	BR3	BR4	BR5	BR6	BR7	BR8	BR9	BR10	Value of Wc	Case no.
Max. temp. [^{0}C]	152.0	132.0	109.0	75.0	57.5	43.0	23.0	24.4	21.7	23.8	15.60	1
Max. res. [ohm]	19.0	28.0	27.3	26.4	25.9	25.6	25.07	50.2	25.04	8.36		
Max. temp. [^{0}C]	87.0	77.0	65.0	47.0	38.0	31.8	21.5	22.25	20.80	21.8	15.52	2
Max. res. [ohm]	17.8	26.5	26.2	25.7	25.5	25.30	25.04	50.10	25.02	8.34		
Max. temp. [^{0}C]	63.0	58.0	51.0	38.0	37.0	27.8	21.0	21.50	20.58	21.1	15.72	3
Max. res. [ohm]	17.4	26.0	25.7	25.4	25.4	25.3	25.03	50.07	25.01	8.34		
Max. temp. [^{0}C]	53.0	48.0	43.0	34.0	29.0	26.0	20.8	21.1	20.45	20.9	15.59	4
Max. res. [ohm]	17.25	25.7	25.5	25.35	25.25	25.15	25.02	50.05	25.01	8.34		
Max. temp. [^{0}C]	47.0	43.0	38.0	31.2	27.8	24.6	20.62	20.9	20.35	20.75	15.72	5
Max. res. [ohm]	17.15	25.6	25.45	25.28	25.20	25.12	25.01	50.05	25.01	8.34		
Max. temp. [^{0}C]	43.0	39.0	35.0	29.2	26.5	23.9	20.5	20.75	20.28	20.6	15.64	6
Max. res. [ohm]	17.05	25.5	25.38	25.22	25.16	25.10	25.01	50.04	25.01	8.34		

TABLE IX
VALUES OF MAXIMUM TEMPERATURE RISE, MAXIMUM RESISTANCE RISE, AND Wc FOR PID-CONTROLLED BR WHEN 1LG FAULT OCCURS AT POINT A

	BR1	BR2	BR3	BR4	BR5	BR6	BR7	BR8	BR9	BR10	Value of Wc	Case no.
Max. temp. [^{0}C]	110.0	109.0	95.0	78.0	62.0	45.0	33.5	53.0	28.5	23.9	16.26	1
Max. res. [ohm]	18.3	27.3	26.9	26.5	26.0	25.64	25.34	51.7	25.2	8.36		
Max. temp. [^{0}C]	68.0	67.0	59.0	51.0	42.0	33.2	27.3	37.0	24.6	21.9	16.45	2
Max. res. [ohm]	17.5	26.2	26.0	25.8	25.55	25.34	25.18	50.83	25.12	8.35		
Max. temp. [^{0}C]	50.0	52.0	46.0	41.0	34.50	29.0	24.9	31.0	23.0	21.2	16.44	3
Max. res. [ohm]	17.2	25.8	25.65	25.5	25.35	25.2	25.12	50.55	25.07	8.34		
Max. temp. [^{0}C]	45.0	43.0	40.0	35.8	31.0	26.7	23.7	28.5	22.4	20.9	16.38	4
Max. res. [ohm]	17.1	25.6	25.5	25.4	25.27	25.17	25.09	50.42	25.06	8.33		
Max. temp. [^{0}C]	40.0	38.0	36.0	32.8	29.0	25.5	22.9	26.7	21.7	20.75	16.40	5
Max. res. [ohm]	17.02	25.48	25.4	25.32	25.22	25.13	25.07	50.33	25.04	8.33		
Max. temp. [^{0}C]	37.0	36.0	34.0	30.5	27.5	24.5	22.6	25.7	21.65	20.65	16.57	6
Max. res. [ohm]	16.95	25.40	25.34	25.27	25.18	25.12	25.06	50.28	25.04	8.33		

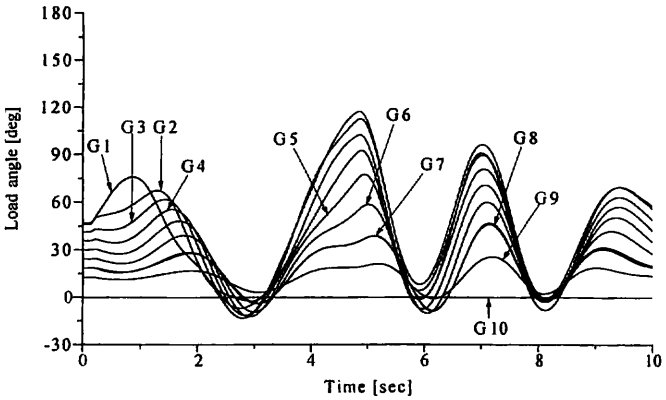

Fig. 17. Load angle responses for PID-controlled BR in case of 3LG fault at point A (simulation case 6 when temperature rise effect is considered).

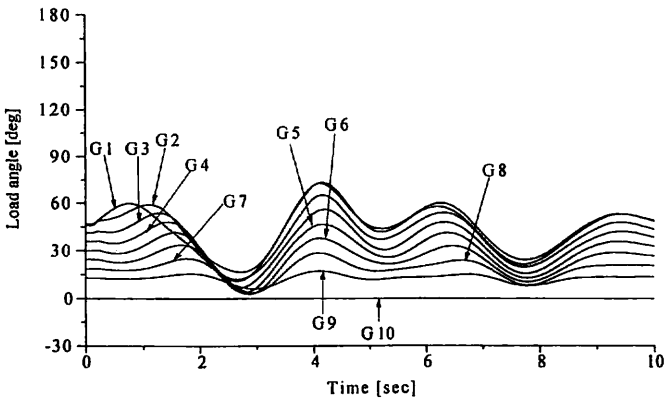

Fig. 18. Load angle responses for fuzzy-controlled BR in case of 1LG fault at point A (simulation case 1 when temperature rise effect is considered).

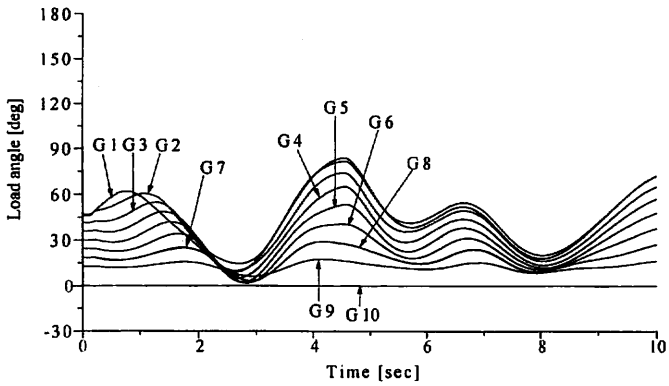

Fig. 19. Load angle responses for PID-controlled BR in case of 1LG fault at point A (simulation case 1 when temperature rise effect is considered).

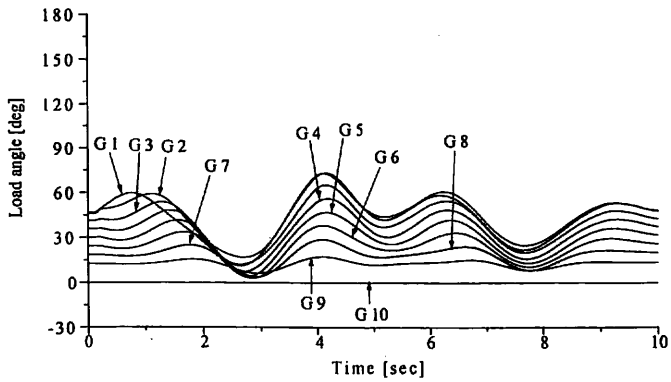

Fig. 20. Load angle responses for fuzzy-controlled BR in case of 1LG fault at point A (simulation case 6 when temperature rise effect is considered).

as shown in Figs. 14–21, considering temperature rise of both fuzzy and PID-controlled BR. This fact also indicates that the temperature change has little or almost no effect on transient stability. Furthermore, it is clearly seen that because of the use of BR, the system is transiently stable for all fault cases. Also, the performance of fuzzy-controlled BR is better than that of PID-controlled BR.

As a whole, from the point of view of the simulation results, several points are of paramount importance.

(a) The fuzzy logic-controlled braking resistor can effectively enhance the transient stability for both balanced and unbalanced faults.

(b) The performance of proposed fuzzy-controlled BR is better than that of PID-controlled BR.

(c) The temperature rise of the braking resistor has little or almost no effect on transient stability.

And overall, the proposed fuzzy-controlled BR provides a simple and effective means of transient stability augmentation in a multimachine power system.

One important thing to note here is that in this work, coherent generators or areas are not determined. However, the fuzzy parameters are fixed for all types of faults and fault locations in the power system. Depending on the faults at different locations

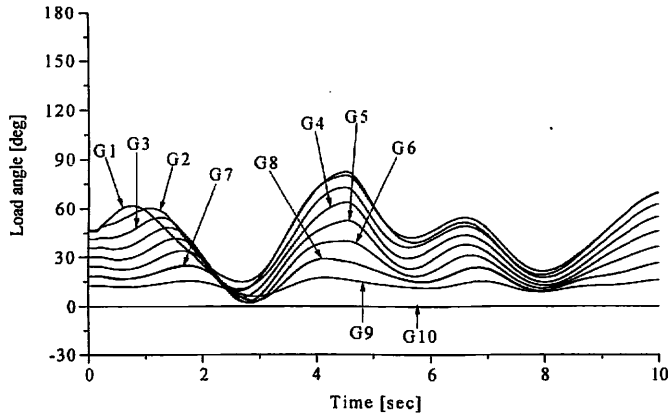

Fig. 21. Load angle responses for PID-controlled BR in case of 1LG fault at point A (simulation case 6 when temperature rise effect is considered).

in the power system, different sets of fuzzy parameters may exhibit good system performance. But practically it is quite uncertain where and what type of fault will occur in a power system. Therefore, the fuzzy logic controller should be installed in the system with only one set of optimal parameters and these parameters cannot be changed during any disturbance in the system. From this viewpoint, only one set of optimal fuzzy parameters is determined by the GA technique and these are applied identically throughout the simulations for all types of faults and fault locations. This fact indicates the robustness of the proposed fuzzy logic controller for the braking resistor switching to improve the transient stability.

VIII. Conclusion

In this paper, a fuzzy logic controller is proposed for the switching of the thyristor-controlled braking resistor to improve the transient stability in a multimachine power system. The temperature rise effect of the braking resistor is included in the simulation. Moreover, the performance of the proposed fuzzy control scheme is compared to that of the conventional PID control scheme. The simulation is implemented by using electromagnetic transients program (EMTP) for both fuzzy and PID control schemes. From the simulation results of both balanced and unbalanced faults at different points, the following conclusions can be drawn:

a) The fuzzy controller can effectively enhance the transient stability by switching the braking resistor.
b) The performance of fuzzy-controlled BR is better than that of PID-controlled BR.
c) The temperature rise of the braking resistor has little or almost no effect on transient stability.
d) The geometry of the braking resistor (i.e., especially its mass and surface area) should be such that the temperature rise is well within the upper temperature limit for the braking resistor material, it is cost-effective and reasonable in size.

It is hoped in future to select the best locations and install a few braking resistors in the system instead of 1 (one) braking resistor at each generator terminal bus which will be sufficient to stabilize the IEEJ West-10 machine model system or any other multimachine model system.

References

[1] Y.-S. Zhou and L.-Y. Lai, "Optimal design for fuzzy controllers by genetic algorithms," *IEEE Trans. Ind. Applicat.*, vol. 36, pp. 93–97, Jan./Feb. 2000.
[2] M. H. Ali, T. Murata, and J. Tamura, "Braking resistor switching by genetic algorithm optimized fuzzy logic controller in multi-machine power system," *Trans. Inst. Elect. Eng. Jpn., Power Energy*, vol. 123-B, no. 3, pp. 315–323, Mar. 2003.
[3] ——, "Transient stability augmentation by fuzzy logic controlled braking resistor in multi-machine power system," in *Proc. IEEE/Power Eng. Soc. Transm. Dist. Conf. Exhibition: Asia Pacific*, 2002, pp. 1332–1337.
[4] M. H. Ali, Y. Soma, T. Murata, and J. Tamura, "A fuzzy logic controlled braking resistor scheme for transient stability enhancement," *Trans. Inst. Elect. Eng. Jpn., Power Energy*, vol. 122-B, no. 1, pp. 113–120, Jan. 2002.
[5] ——, "A fuzzy logic controlled braking resistor scheme for stabilization of synchronous generator," in *Proc. IEEE Int. Elect. Mach. Drives Conf.*, 2001, pp. 548–550.
[6] Bulk Power System Models *http://www.pwrs.elec.waseda.ac.jp/powsys/english/kikan/* [Online]
[7] D. F. Peelo, D. W. Hein, and F. Peretti, "Application of a 138 KV 200 MW braking resistor," *Power Eng. J.*, vol. 8, no. 4, pp. 188–192, Aug. 1994.
[8] A. J. Chapman, *Fundamentals of Heat Transfer*. New York: Macmillan, 1987, p. 14.
[9] Initial Value Problems for Growth and Decay, UBC Calculus Online Course Notes *http://www.ugrad.math.ubc.ca/cousedoc/math100/notes/diffeqs/cool.html* [Online]
[10] D. Driankov, H. Hellendoorn, and M. Reinfrank, *An Introduction to Fuzzy Control*. New York: Springer-Verlag, 1993, pp. 89–209.
[11] P. N. Paraskevopoulos, *Digital Control Systems*. Englewood Cliffs, NJ: Prentice-Hall, 1996, pp. 139–144.
[12] D. E. Goldberg, *Genetic Algorithms in Search, Optimization, and Machine Learning*. Reading, MA: Addison-Wesley, 1989.
[13] Z. Michalewicz, *Genetic Algorithms + Data Structures = Evolution Programs*. New York: Springer-Verlag, 1994.
[14] "IEEE standard for synchrophasors for power systems," *IEEE Trans. Power Delivery*, vol. 13, pp. 73–77, Jan. 1998.
[15] H. Y. Li, E. P. Southern, P. A. Crossley, S. Potts, S. D. A. Pickering, B. R. J. Caunce, and G. C. Weller, "A new type of differential feeder protection relay using the global positioning system for data synchronization," *IEEE Trans. Power Delivery*, vol. 12, pp. 1090–1097, July 1997.
[16] R. E. Wilson, "Methods and uses of precise time in power systems," *IEEE Trans. Power Delivery*, vol. 7, pp. 126–131, Jan. 1992.
[17] M. Yagami, S. Shibata, T. Murata, and J. Tamura, "Improvement of power system transient stability by superconducting fault current limiter," in *Proc. IEEE/Power Eng. Soc. Transm. Dist. Conf. Exhibition: Asia Pacific*, 2002, pp. 359–364.

Mohd. Hasan Ali (S'00) received the B.Sc. Eng. degree in electrical engineering from Bangladesh Institute of Technology (BIT)-Rajshahi, Bangladesh, and the M.Sc. Eng. degree in electrical engineering from Kitami Institute of Technology, Hokkaido, Japan, in 1995 and 2001, respectively. He is currently pursuing the Ph.D. degree at the Kitami Institute of Technology.

Currently, he is a Lecturer in the Electrical and Electronic Engineering Department of BIT- Rajshahi, Bangladesh.

Mr. Ali is a student member of the IEE of Japan.

Toshiaki Murata completed his Electrical Engineering Curriculum of the Teacher Training School from Hokkaido University, Hokkaido, Japan. He received the Dr. Eng. degree from Hokkaido University in 1991.

Currently, he is an Associate Professor at the Kitami Institute of Technology, Hokkaido, Japan, where he was a Research Assistant since 1969.

Dr. Murata is a member of the IEE of Japan and Society of Instrument and Control Engineers of Japan.

Junji Tamura (SM'92) received the B.Sc. Eng. degree in electrical engineering from Muroran Institute of Technology, Hokkaido, Japan, in 1979, and the M.Sc. Eng. and Dr. Eng. degrees in electrical engineering from Hokkaido University, Hokkaido, Japan, in 1981 and 1984, respectively.

Currently, he is a Professor at the Kitami Institute of Technology, Hokkaido, Japan. He became a Lecturer in 1984 and an Associate Professor in 1986 with the Kitami Institute of Technology.

Dr. Tamura is a member of the IEE of Japan.